Macromolecules
ARTICLE

*Macromolecules* **2009**, *42*, 9027–9033 **9027**
DOI: 10.1021/ma9016345

# Polystyrene−Polylactide Bottlebrush Block Copolymer at the Air/Water Interface

**Lei Zhao,[†] Myunghwan Byun,[†] Javid Rzayev,[‡] and Zhiqun Lin*,[†]**

[†]*Department of Materials Science and Engineering, Iowa State University, Ames, Iowa 50011, and* [‡]*Department of Chemistry, University at Buffalo, The State University of New York, Buffalo, New York 14260-3000*

*Received July 23, 2009; Revised Manuscript Received September 17, 2009*

ABSTRACT: Hydrophobic ultrahigh molecular weight bottlebrush block copolymer and linear block copolymer of polystyrene−polylactide (PS−PLA) were shown to be capable of forming Langmuir monolayers and exhibiting unique assembly behaviors at the air/water interface, which cannot be addressed by the classic theory of Langmuir monolayer of amphiphilic copolymers. New models were proposed to illustrate these intriguing surface behaviors. The self-assembled structure of Langmuir monolayer of bottlebrush block copolymer was determined by a combination of AFM measurement, thermal annealing, and enzymatic degradation experiment. To the best of our knowledge, this is among few studies on hydrophobic block copolymers at the air/water interface. As such, it not only complements the well-known models of self-assembly of amphiphilic block copolymers at the air/water interface but also expands the use of Langmuir−Blodgett (LB) technique to hydrophobic block copolymers.

## Introduction

As one of the most typical film preparation methods, the Langmuir−Blodgett (LB) technology has been widely utilized to produce copolymer films with mono- or multimolecule layers.[1] These copolymer films with well-controlled thickness have been attracting considerable attention due to their broad range of potential applications in microlithography,[2] devices,[3] and biomimetic thin films.[4] The overall property of these copolymer Langmuir films is closely related to their surface morphology, which is dictated by a number of parameters, including the solution concentration, surface pressure, and temperature.[2,5−7]

The interfacial behavior of amphiphilic copolymers at the air/water interface has been extensively studied since the pioneering work of Eisenberg and Lennox.[5,8−10] The so-called "pancake" and "brush" models have been established and proved quite effective in understanding the air/water interfacial behavior of a variety of amphiphilic copolymers, such as linear block copolymers,[2,6,7,11,12] star copolymers,[13−17] comb block copolymers,[18] dendritic polymers,[19−21] etc. The "pancake" model refers to the morphology of copolymer LB film formed at low surface pressure. In this model, the hydrophilic blocks spread over the water surface, forming the pancake-like morphology, while the hydrophobic blocks aggregate and sit on the hydrophilic "pancake" to reduce the surface energy. Under higher compression pressure, the "pancake" is transformed into the "brush"; i.e., the spread hydrophilic blocks are expelled into the water subphase, yielding brush-like morphology ("brush" model). To date, only few hydrophobic copolymers, for example PS−PMMA[22−24] and PI−PMMA,[25] have been reported to form LB monolayer in which neither block is water-soluble; these copolymers have surface active blocks with hydrophilic groups (e.g., ester group in PMMA[26]), thereby possessing a relatively strong affinity on the water surface as amphiphilic copolymers. As discussed above, the presence of hydrophilic or water surface active blocks is essential for the formation of Langmuir monolayer because they facilitate the tethering of whole copolymer chain on the water surface. So far, self-assembly of LB films has been primarily focused on amphiphilic copolymers. By contrast, few studies on hydrophobic copolymers at the air/water interface have been pursued, and they were mainly limited to linear copolymers.[22−25] In this paper, both bottlebrush and linear block copolymers of hydrophobic polystyrene−polylactide were found, for the first time, to be capable of forming the Langmuir monolayers on the water surface. The systematic studies showed that they displayed unique assembly behaviors at the air/water interface, which can no longer be understood by the classic models for amphiphilic copolymers as well as by the previously reported models of linear hydrophobic copolymers.

The polystyrene−polylactide (PS−PLA) block copolymers were selected in the present study because of the biodegrable nature of PLA blocks.[27] Thin films of these copolymers are promising in biomedical and pharmaceutical application.[28] Notably, all previous research on PS−PLA block copolymers are limited in their self-assembly in bulk and thin films,[29−32] and no self-assembly of Langmuir monolayer has ever been reported. Recently, a novel ultrahigh molecular weight PS−PLA bottlebrush block copolymer (BBCP) was synthesized by a combination of living radical and ring-opening polymerizations.[29] PS−PLA BBCP is a comb-like macromolecule with highly densely grafted PS and PLA branches along the polymethacrylate backbone. The backbone is much longer than the branches. The steric effect of adjacent branches causes the backbone to stretch out, leading to the formation a rigid cylindrical macromolecule as illustrated in Figure 1a.[29,33,34] Furthermore, the densely branched structure and large cross-sectional area of cylindrical shape of BBCP result in little entanglement between the BBCP melts.[34,35] The unique properties described above, together with their large domain size and domain spacing originating from the ultrahigh molecular weight of BBCP, make BBCP a perfect candidate to explore their self-assembly behavior at the air/water interface.

*To whom correspondence should be addressed. E-mail: zqlin@iastate.edu.



Published on Web 09/28/2009

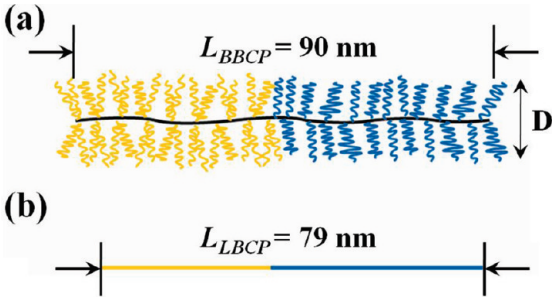


**Figure 1.** Schematic representations of (a) a newly synthesized bottlebrush copolymer (BBCP) with PLA (yellow) and PS (blue) chains densely grafted on the backbone (black) and (b) a fully stretched linear block copolymer (LBCP) of PS-*b*-PLA, in which PLA and PS blocks are in yellow and blue, respectively. The length and diameter of block copolymers are labeled in the schematic.

In this paper, the Langmuir isotherms and surface morphologies of BBCP were presented. The structure of deposited LB films of BBCP was then determined by the AFM measurements, thermal annealing, and enzymatic degradation experiments. A linear block copolymer (LBCP) of PS−PLA with relatively similar molecular length and composition ratio to BBCP was employed and served as the reference to elucidate the influence of chemical architecture on the air/water interfacial behavior of PS−PLA Langmuir monolayers (Figure 1b). Combined with the study of PS−PLA LBCP, the surface behavior of PS−PLA block copolymer systems at the air/water interface was finally revealed.

## Experiment

Previously synthesized PS−PLA BBCP with an ultrahigh molecular weight (MW) of 1 200 000 g/mol was utilized in the study.[29] PS−PLA LBCP with MW of 34 000 g/mol and PS volume fraction of 71.4% was synthesized according to a literature procedure.[36] The dimension of PS−PLA BBCP was estimated from molecular model by performing energy minimization using Material Studio 4.1. The length of PS−PLA LBCP in fully stretched state was also estimated from molecular model. Chloroform (99.9%, Fisher Chemicals) and Proteinase K (Sigma, lyophilized powder) were purchased and used without further purification. The BBCP and LBCP chloroform solutions at a concentration $c = 2 \times 10^{-3}$ g/mL were prepared, and a 12 $\mu$L solution was placed on the LB trough for each experiment. Surface pressure−area ($\pi$−$A$) isotherms of block copolymer monolayers were obtained with the R&K Langmuir−Blodgett (LB) system (Riegler & Kirstein, GmbH, 160 $cm^2$ Teflon trough). Before LB deposition, the LB trough was carefully cleaned with 1:1 $H_2O_2$:$NH_3OH$ solution overnight and subsequently rinsed with DI water (NanoPure, >18 MΩ cm) five times. After chloroform evaporated for 30 min, the monolayer film was compressed at a rate of 150 $\mu$m/s.

Si substrate used for depositing LB films was cleaned with a mixture of sulfuric acid and Nonchromix, followed by rinsing with DI water and blown dry with $N_2$. For LB depositions, the Si substrate was withdrawn at a rate of 35 $\mu$m/s while keeping the pressure constant. The scratch experiment was carried out by gently mechanically removing the deposited LB film with a blade. Thermal annealing of deposited films was conducted in an oven at the desired temperature for a certain amount of time. The enzymatic degradation was performed by vertically immersing the deposited LB film into the degradation solution, which was prepared by adding 1.0 mg of Proteinase K into 5 mL of Tris-HCl buffer (pH = 8.6) at 37 °C for 1 h in an oil bath.

Morphologies of LB films were examined by atomic force microscopy (AFM; Dimension 3000) in the tapping mode. The scanning rate was 2 Hz. Each sample was imaged at more than five locations to ensure the reproducibility of features observed. The interdomain distance was obtained by performing 2D fast Fourier transform (FFT) of the AFM height images. The aggregation number of the domains was estimated by the surface area of domains and arms obtained from the AFM images divided by the molecular area obtained from the isotherm.

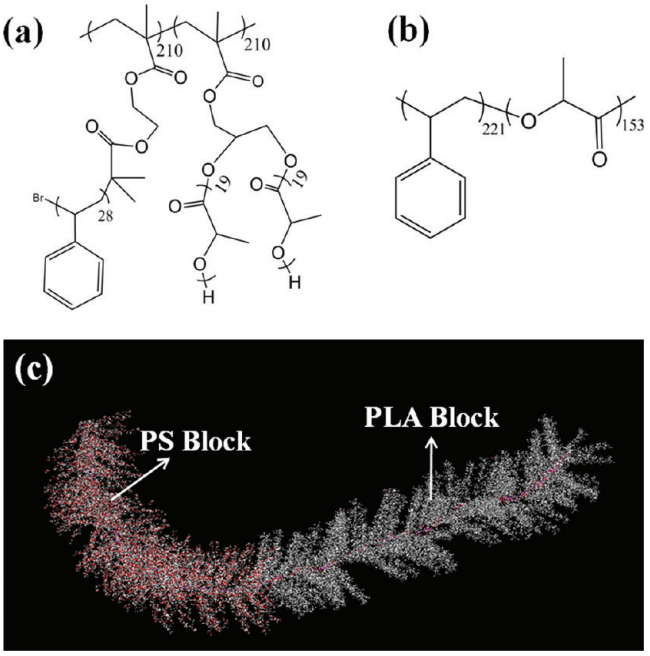


**Figure 2.** Chemical structures of (a) bottlebrush copolymer (BBCP) and (b) PS-*b*-PLA linear block copolymer (LBCP). (c) Molecular morphology of BBCP established by Material Studio 4.1, in which PS and PLA chains are labeled in red and gray, respectively.

## Results and Discussion

The chemical structure and molecular morphology of PS−PLA BBCP are depicted in Figure 2a,c. A detailed information on BBCP can be found in our previous work.[29] The PS (red) and PLA (white) branches are densely grafted along the polymethacrylate backbone through the ester group. The backbone can be divided into two parts with the same length, namely, one grafted with PLA arms (i.e., PLA part) and the other grafted with PS arms (i.e., PS part). The volume fraction of PS is calculated to be 60% using the known densities of $\rho_{PS}$ = 1.04 and $\rho_{PLA}$ = 1.25 g/mL. The length of BBCP backbone, $L_{BBCP}$, was about 90 nm (Figure 1a), and the lengths of PLA and PS arms are 6.3 and 6.5 nm (Figure S1), respectively, obtained by performing energy minimization at room temperature using Material Studio 4.1. Because of steric crowding of PLA and PS arms, the BBCP adopts a relatively rigid cylindrical morphology in the solid state, with the aspect ratio of the length to diameter, $L/D$ = 9 (Figure 1a). The chemical structure of PS−PLA LBCP is shown in Figure 2b; the MW of PS and PLA blocks are 23 000 and 11 000 g/mol, respectively. The LBCP assumes a random coil conformation in both the chloroform solution and the melt state due to the absence of the steric effect of arms as in the case of BBCP. The length of a fully stretched LBCP is estimated to be 79 nm with PS block of 45 nm and PLA block of 34 nm (Figure 1b).

Langmuir isotherm (i.e., surface pressure−area, $\pi$−$A$, plot) of the BBCP is shown in Figure 3a. The continuous pressure rise indicated the formation of Langmuir monolayer.[1] The entire isotherm can be divided into three typical regions based on the slope of the isotherm (i.e., the pressure increasing rate with the molecular area).[1,5] They are (i) gas state region at $\pi$ = 0 mN/m, (ii) liquid state region at $\pi$ = 0−13 mN/m, and (iii) condensed state region at $\pi$ > 13 mN/m. Figure 4 shows the representative

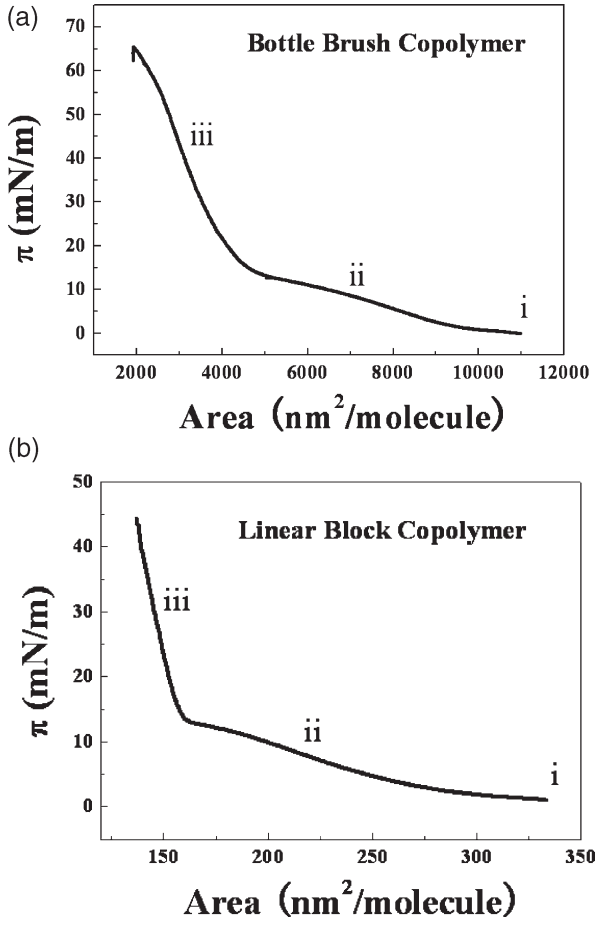


**Figure 3.** Pressure−area isotherms of the Langmuir monolayer of (a) BBCP and (b) LBCP. Three regions are labeled as (i) gas state, (ii) liquid state, and (iii) condensed state.

AFM height images of Langmuir monolayers obtained at $\pi$ = 1, 5, 13, and 30 mN/m; dot-like domains with a broad size distribution were observed. Table 1 summarizes the domain height, size, and their surface and aggregation number. With the increase in surface pressure, the domain shape and the aggregation number of the domains did not show obvious change; however, the number of domains dramatically increased with the surface coverage increasing from 29.84% at $\pi$ = 1 mN/m to 66.12% at $\pi$ = 30 mN/m. Moreover, the initially dispersed dot-like domains transformed into the island-like morphology at the condensed state region (i.e., region iii). It is noteworthy that the domain height, however, showed little difference at different surface pressures (Table 1).

At the first glance, the LB isotherm and dot-like morphology of BBCP resembled those of amphiphilic block copolymers;[5,15,21] the latter assumes the "pancake" morphology on the water surface (i.e., the hydrophobic blocks aggregate into dot-like domains with the hydrophilic blocks forming the spreading phase surrounding the hydrophobic blocks). However, the fact that no domain height difference was observed at different surface pressures cannot be explained by the models of amphiphilic copolymers that are described previously. According to the theory of amphiphilic copolymers at the air/water interface, the domain height should be largely increased with the increase in surface pressure due to the formation of brush-like structure.[5,11] Thus, to fully understand the surface behavior of the hydrophobic BBCP, it is necessary to systematically explore the fine structure of dot-like domains, which was revealed via a combined study of AFM measurement through a mechanical scratching test, thermal annealing, and enzymatic degradation.

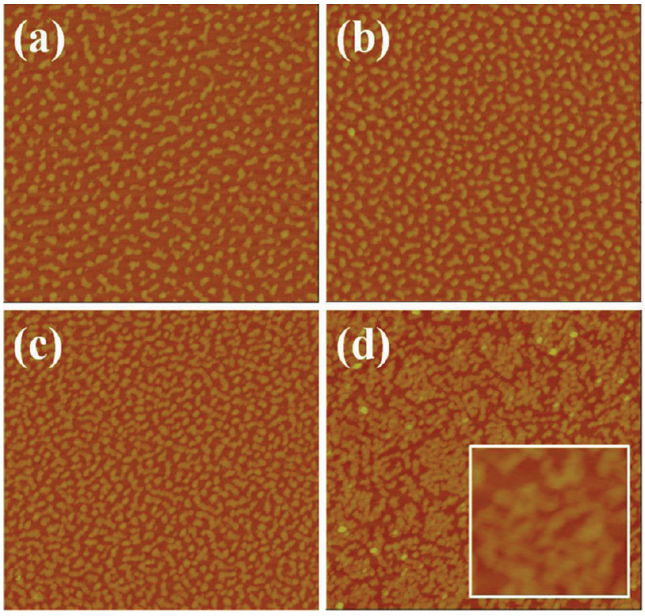


**Figure 4.** AFM height images of the BBCP Langmuir monolayers obtained from the chloroform solution at various transfer pressures: (a) $\pi$ = 1 mN/m, (b) $\pi$ = 5 mN/m, (c) $\pi$ = 13 mN/m, and (d) $\pi$ = 30 mN/m. Chloroform was allowed to evaporate for 30 min before the LB deposition. Scan size = 3 $\mu$m × 3 $\mu$m and $z$ scale = 50 nm for all images. Scan size = 0.5 $\mu$m × 0.5 $\mu$m for the inset in (d).

**AFM Study.** The LB film deposited at $\pi$ = 5 mN/m was gently scratched with a razor blade to remove a small portion of the film and subsequently examined with AFM (Figure 5). The section analysis showed that the height difference between the exposed Si substrate and the interdomain region in the LB film was about 0.7 nm (Figure S2). The result suggested that a spreading phase should exist between the dot-like domains; this is reasonable because no surface pressure can be applied on the LB film if the space between the dot-like domains was empty (i.e., not occupied by the spreading phase). This was further revealed in the AFM phase images (Figure 5b,c), in which the spreading phases (i.e., arm in Figure 5c) surrounding the dot-like domain (i.e., domain in Figure 5c) were clearly evident. In AFM phase images taken in the tapping mode, the magnitude of phase shift is directly related to the elastic modulus of the sample.[37] As shown in Figure 5b,c, two distinct phases in the LB film can be readily discriminated; one phase, composed of the dot-like domain, appeared dark, and the other appeared light and was in the form of cylindrical arms surrounding the dark domains, which constituted the spreading phase. These arms were closely connected to the dot-like domain radially (Figure 5c). Moreover, the aggregation number of the domains estimated from isotherm and AFM images was ~11, which is in good agreement with the PLA arms (~10) observed in Figure 5c. To the best of our knowledge, this is the first time the morphology of spreading phases is observed by a microscopy technique. The length and width of the arm were 40 and 20 nm, respectively. Considering the twisting of polymer backbones,[29] these arms had the similar length to one part of BBCP, either the PS part or the PLA part described previously. It has been reported that both PS[38] and PLA[39] are able to form the spreading phase at the air/water interface. Therefore, to identify which part of BBCP composed the dot-like domain and the other formed the spreading phases adjacent to it, thermal annealing study was performed.

**Thermal Annealing.** The molecular weights (MWs) of PS and PLA branches in the PS−PLA BBCP are 3000 and 1400 g/mol, respectively, which are smaller than their critical

**Table 1. Height, Size, and Surface Coverage of BBCP Dot-like Domains Obtained from AFM Images**

| | $\pi$ = 1 mN/m | $\pi$ = 5 mN/m | $\pi$ = 13 mN/m | $\pi$ = 30 mN/m |
|---|---|---|---|---|
| domain height (nm) | 3.67 ± 0.69 | 3.93 ± 0.87 | 3.64 ± 0.67 | 3.82 ± 0.89 |
| domain size (nm) | 68.75 ± 8.20 | 66.72 ± 7.79 | 66.07 ± 4.87 | |
| surface coverage (%) | 29.84 | 37.95 | 53.00 | 66.12 |
| aggregation number of domains | 11 | 11 | 14 | |

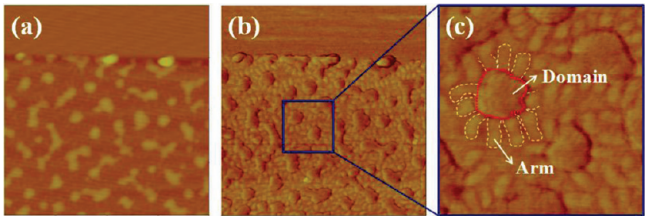


**Figure 5.** (a) AFM height image of the BBCP Langmuir monolayer obtained after scratching off the top portion of monolayer. Scan size = 1 $\mu$m × 1 $\mu$m and $z$ scale = 50 nm. (b) The corresponding phase image of (a). Phase scale = 50°. (c) Close-up of the phase image in (b); the domain is enclosed with red dash line and arms with white. Scan size = 0.3 $\mu$m × 0.3 $\mu$m and phase scale = 50°. The original Langmuir monolayer was obtained at $\pi$ = 5 mN/m.

entanglement MWs, that is, 14 000 g/mol for PS[40] and 4000 g/mol for PLA.[41] Thus, the whole BBCP molecules should be mostly free of entanglements above its glass transition temperature, $T_g$.[29,34,35] DSC measurement showed that the BBCP had two well-defined $T_g$s at 54 and 104 °C, corresponding to the $T_g$ of PLA and PS, respectively.[29] Two LB films deposited at $\pi$ = 5 mN/m were annealed at 95 °C for 12 h and 170 °C for 5 h. Figure 6 shows AFM images of annealed samples. The dot-like domain height was labeled in each height image. The interdomain distance, $\lambda_{C-C}$, analyzed by performing 2D fast Fourier transform of the height images, was 124.6 ± 29.4 and 119.8 ± 28.1 nm for the original sample (Figure 6a) and annealed sample at 95 °C (Figure 6c), respectively. The domain height, however, remained the same, and the shape of the arms was well maintained as evidenced in the phase image (Figure 6d). On the basis of these observations, it is clear that no obvious changes occurred after thermal annealing at 95 °C, which was far above the $T_g$ of PLA. However, when annealed at 170 °C, a temperature well above the $T_g$ of PS, the domain height markedly decreased, and the phase image was dramatically changed (Figure 6f). Taken together, these results suggest that the originally formed dot-like domain consist of the PS part of BBCP, while the arm-like structures were formed by the PLA part. When annealed at 170 °C, the PS chains within the PS part of BBCP became mobile. This led to the separation of PS chains from one another and subsequent merging with separated PS chains from the neighboring PS part to yield a continuous PS phase, as shown in Figure 6f.

It is worth noting that, as schematically illustrated in Figure 7, there are two different means by which the polymer blocks can be arranged to yield the images observed in Figures 5 and 6. In model A, the domains are composed of the PS part (i.e., PS domain), which are separated by the spreading PLA part (i.e., PLA arms). By contrast, in model B, the PLA arms situate around the PS domain as well as beneath it; in other words, the PS domain sits on the top of a continuous PLA layer. In order to determine which model is appropriate for the self-assembly of PS−PLA BBCP at the

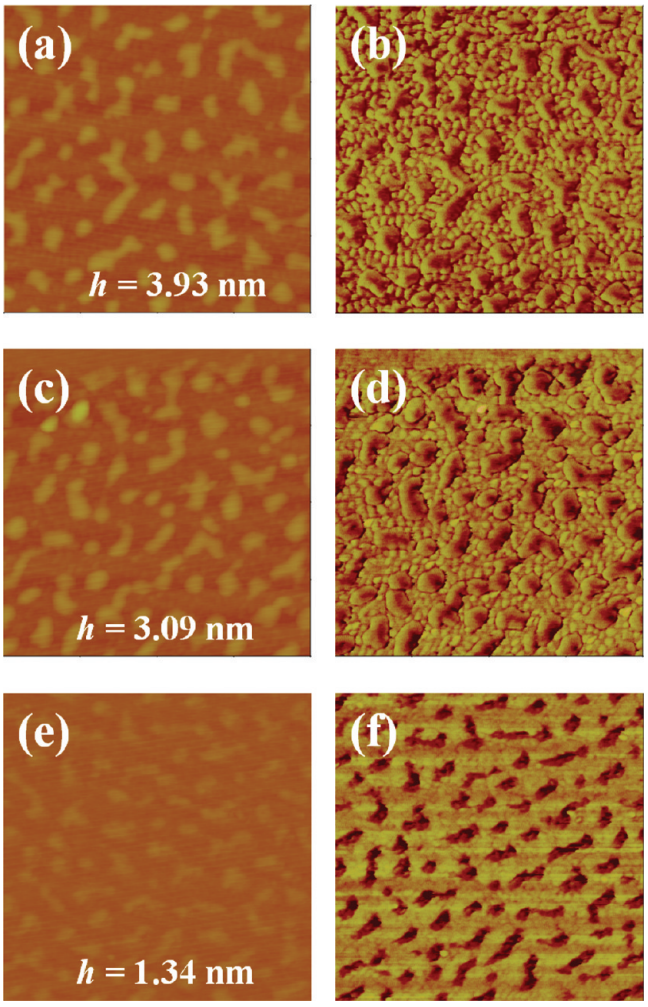


**Figure 6.** AFM height and phase images of (a, b) original Langmuir monolayer, (c, d) monolayer annealed at 95 °C for 12 h, and (e, f) monolayer annealed at 170 °C for 5 h. (a), (c), and (e) are height images and (b), (d), and (f) are phase images. Scan size = 1 $\mu$m × 1 $\mu$m, $z$ scale = 50 nm, and phase scale = 50°. The original Langmuir monolayer was obtained at $\pi$ = 5 mN/m.

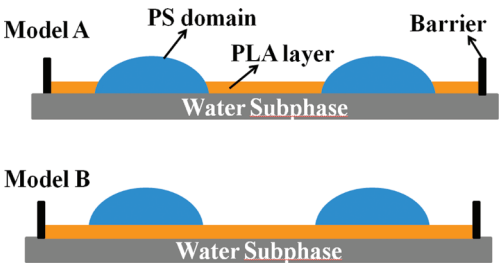


**Figure 7.** Schematic illustration of two models PS-*b*-PLA block copolymer at the air/water interface.

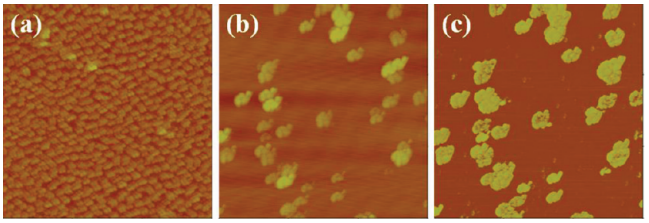


**Figure 8.** (a) AFM height image of Langmuir monolayer after immersion in the buffer solution without the addition of enzyme for 1 h. (b) AFM height image of Langmuir monolayer undergoing enzymatic degradation for 1 h. (c) Corresponding phase image of (b). Scan size = 3 $\mu$m × 3 $\mu$m, $z$ scale = 50 nm, and phase scale = 50°. The original Langmuir monolayer was obtained at $\pi$ = 5 mN/m.

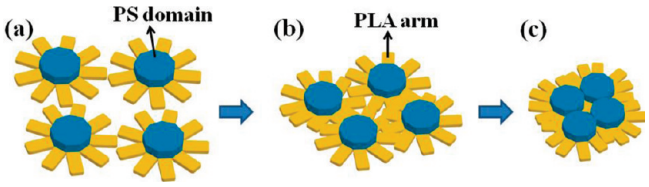


**Figure 9.** Schematic stepwise representation of the packing of microstructures of BBCP: (a) at the low pressure (i.e., between regions i and ii), where PLA arms (yellow) highly spread over the water surface and PS (blue) form domains on the top of PLA; (b) at the intermediate pressure (i.e., region ii), where the rearrangement of PLA arms occur; and (c) at the high pressure (i.e., region iii), where the PLA arms are highly compressed and PS domains become connected.

air/water interface seen in Figures 5 and 6, an enzymatic degradation study was conducted.

**Enzymatic Degradation.** The motivation of this study was to selectively degrade PLA blocks in the LB film; thus, the precise location of the PLA phase can be identified. PLA is a biodegradable polymer which can be degraded by either an enzymatic approach or alkaline hydrolysis.[27,42] Given the fact that the alkaline hydrolysis may cleave the ester groups that connected the PS branches to the backbone, enzymatic degradation using Proteinase K was performed instead, thereby keeping the PS part intact. As shown in Figure 8a, the dot-like domain morphology was retained after being soaked in the Tris-HCl buffer solution for 1 h. The morphology was a little blurry, which may be due to the swelling effect of water or the shearing effect when the LB film was withdrawn from the buffer solution. By contrast, after degradation with Proteinase K for 1 h, although the circular domain existed, they gathered together to yield large aggregates, leaving behind nothing in the region between the aggregates (Figure 8b,c). The enzymatic degradation result, first of all, confirmed the fact that the dot-like domain was made up of the PS part; otherwise, it would have degraded and dissolved in buffer. More importantly, this result suggests that for the self-assembly of PS−PLA block copolymers at the air/water interface model B is the mechanism that underpinned the observed morphologies in Figures 5 and 6. According to model A, when PLA phases are removed by enzymatic treatment, the PS domains should be well retained on the Si substrate. In marked contrast, if the LB film adopts the arrangement depicted in model B, the PS domains can be readily stripped off the substrate after degrading PLA beneath them. Since water has a strong wetting ability on the Si substrate,[43] a water layer may thus form on the Si substrate during the PLA degradation. The decreased interaction between the Si substrate and PS can lead to the aggregation of PS domains which was composed of dot-like domains of the same size as that of freshly deposited LB film (Figure 5b). Thus, we believe that model B better describes the morphology of the self-assembled PS−PLA BBCP monolayers at the air/water interface.

**Interfacial Behavior of PS−PLA Block Copolymer.** Upon the evaporation of chloroform in the gas state region ($\pi$ = 0 mN/m), the PS part of BBCP aggregated, forming the dot-like domains to reduce its surface energy (Figure S3), where only extremely small PS domains exist in the LB film. Although PLA is a hydrophobic polymer,[39] it contains ester groups, which enables the formation of hydrogen bonds with water and results in attractive interaction between PLA and water subphase as compared to PS.[39] Therefore, the PLA part spread over the water subphase, contacted with one another, and prevented the PS parts from aggregating. A monolayer was thus formed at low pressure (Figure 9a). With the increase in surface pressure (i.e., in the liquid state region ii in Figure 3a), there was a strong elastic repulsive force between the PLA parts; this is analogous to the behavior of spreading phase in amphiphilic block copolymers.[5,10] As a result, a continuous pressure increase was observed in this region. However, due to the intrinsic hydrophobic nature of PLA,[39] it can hardly be expelled into the water subphase to form brush-like morphology as commonly seen in amphiphilic block copolymers. Thus, PLA arms that surrounded the PS domain had to rearrange themselves to release the elastic stress (Figure 9b). The surface area of the spreading PLA phases was largely decreased via interdigitation, leading to the increased density of dot-like domains (Figure 9b). Finally, the PLA arms were strongly compressed in the condensed state region (Figure 9c). The condensed LB film was incompressible, and the surface pressure increased dramatically with little decrease of the molecular area (i.e., region iii in Figure 3a). Under this high surface pressure, the PLA arms were expelled apart (Figure 9c); the PS domains became connected, yielding an island-like morphology (Figure 4d). Because certain PLA arms may still exist between the PS domains, the PS domains in the island was loosely packed as shown in the inset of Figure 4d. By contrast, under high surface pressure, amphiphilic block copolymers form more continuous island morphology, as the spreading phase was completely expelled into water subphase.[44]

To explore the effect of bottlebrush structure on the formation of LB films, a linear block copolymer (LBCP) of PS−PLA with close molecular length and composition ratio to BBCP was investigated for comparison. The LBCP had similar shape of the pressure−area isotherm as that of BBCP, indicating that LBCP has similar assembly behavior at the air/water interface as BBCP. The only difference was the area per molecule; this is due to the size difference of two copolymers. The AFM images of Langmuir monolayers of LBCP obtained at different pressures are shown in Figure 10. As evidenced in Figure 10a, dot-like domains with relatively well-defined shape originating from the flexible nature of LBCP chains were observed; the domain size and height are 59 and 3.35 nm, respectively, similar to that of BBCP at the same surface pressure (i.e., 68.75 and 3.67 nm, respectively; $\pi$ = 1 mN/m). Because of higher volume fraction of PS block in LBCP (i.e., 71.4%) than in BBCP (i.e., 60%), the PS domains in LBCP were found to have a large surface coverage of 37.36% compared to 29.84% in BBCP. No arm-like structures were seen in the phase image (Figure 10b); this is because the linear PLA blocks are flexible and their MW of 11 000 g/mol is higher than the critical MW of 4000 g/mol for entanglement.[41] Thus, the PLA blocks entangled and spread on the water surface (Figure 11a). On the other hand, bottlebrush PLA blocks in BBCP are rigid and have a large

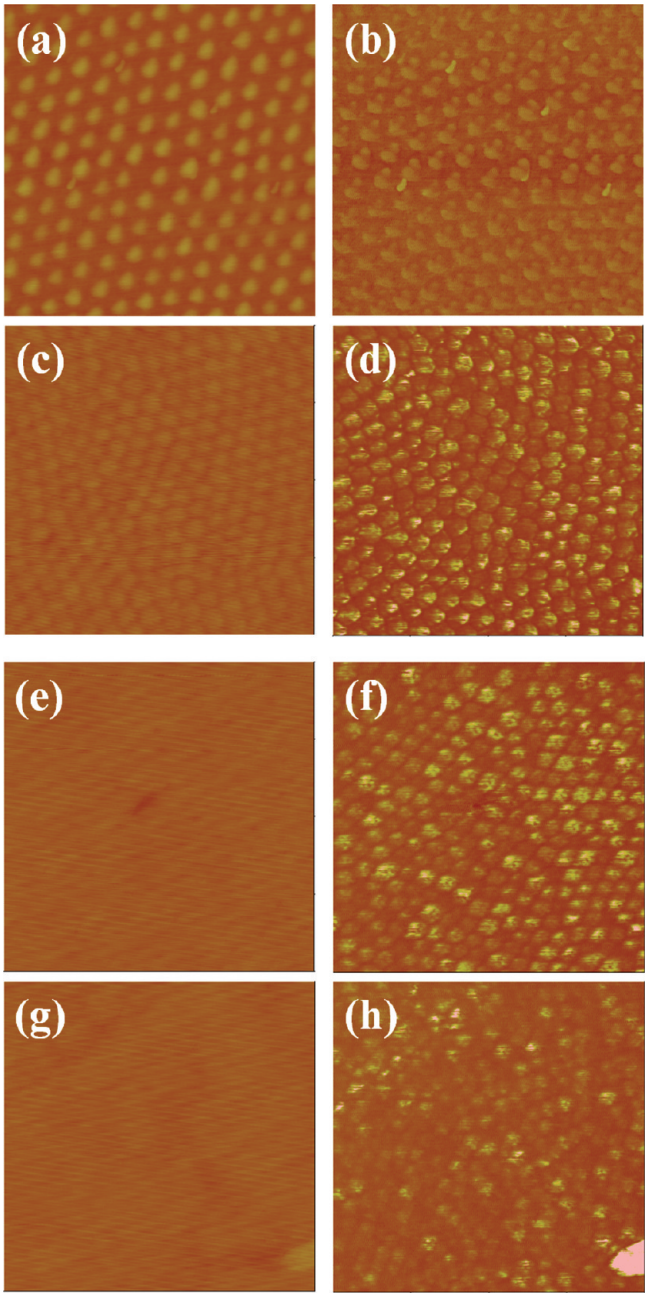


**Figure 10.** AFM height images (a, c, e, and g) and corresponding phase images (b, d, f, and h) of Langmuir monolayers of PS-*b*-PLA LBCP obtained from the chloroform solution at various surface pressures: (a) and (b) $\pi$ = 1 mN/m, (c) and (d) $\pi$ = 5 mN/m, (e) and (f) $\pi$ = 13 mN/m, and (g) and (h) $\pi$ = 30 mN/m. Chloroform was allowed to evaporate for 30 min before the LB deposition. Scan size = 1 $\mu$m × 1 $\mu$m, *z* scale = 30 nm, and phase scale = 50°.

cross-sectional area so that they can be readily visualized by AFM (Figures 1a, 5, and 6).

At $\pi$ = 5 mN/m, the domain height of LBCP dramatically decreased as seen in the AFM height image (Figure 10c). This contrast sharply with amphiphilic copolymers[11] and the BBCP in the present study; the latter showed little change in the domain height as the pressure increased (Table 1). The decrease of domain height can be attributed to the folding of flexible PLA chains (Figure 10c). The folding process of PLA chains have been reported on the assembly of linear PLA−PEO block copolymer at the air/water interface.[39] Because of the folding of PLA chains as a result of applied

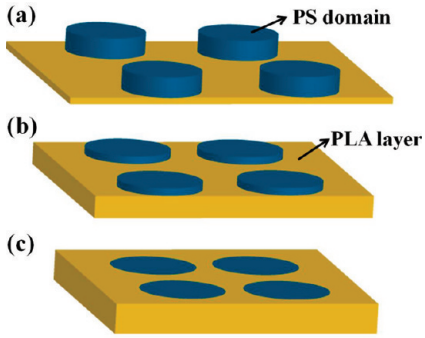


**Figure 11.** Schematic illustration of the packing of microstructures of PS-*b*-PLA LBCP at different surface pressures: (a) at the low pressure (i.e., between regions i and ii), where PLA arms (yellow) highly spread over the water surface and PS (blue) form domains on the top of PLA); (b) at the intermediate pressure (i.e., region ii), where the folding of PLA chains lead more PLA to occupy the space between PS domains; and (c) at the high pressure (i.e., region iii), where the folding of PLA chains is complete, thereby leading to the formation of a topologically continuous film.

compressive surface pressure, the surface stress was released and the space between PS domains was filled with PLA chains, thereby leading to the reduction in the height difference between the PS domain and the spreading PLA phase (Figure 11b). At high pressure, $\pi$ = 13 mN/m, the folding of PLA chains may be completed (Figure 11c), and the inter-domain space was fully occupied by PLA chains. Consequently, a smooth surface of LBCP Langmuir monolayer was yielded (Figure 10e); however, the light PS domain and the dark PLA phase can still be readily resolved in the corresponding phase image (Figure 10f). In the case of BBCP, the PLA bottlebrushes cannot be folded due to the present of rigid backbone; thus, the PS domains were still highly dispersed at $\pi$ = 13 mN/m (Figure 4c), and no variation in the domain height was observed (Table 1). At very high pressure, $\pi$ = 30 mN/m, the LBCP LB film was highly compacted (Figure 10g,h), and the surface pressure dramatically increased with a slight decrease of molecular area (region iii in Figure 3b).

## Conclusions

In summary, we systematically studied the air/water interfacial behavior of newly synthesized, ultrahigh MW bottlebrush as well as linear PS−PLA block copolymers. These hydrophobic block copolymers exhibited unique self-assembly as a function of surface pressure at the air/water interface. The self-assembled structure of a Langmuir monolayer of bottlebrush block copolymer was determined by combining the studies of AFM measurement, thermal annealing, and enzymatic degradation. The influence of chemical architecture on assembly behavior of PS−PLA Langmuir monolayer at the air/water interface was also explored. Rather than undergoing "pancake" to "brush" transition as commonly seen in amphiphilic block copolymers, for the PS−PLA BBCP, the pancake-like morphology formed at the low pressure transformed into interdigitated and eventually island-like morphology at the high pressure; the height of domains in the Langmuir monolayer was unchanged despite the increase in surface pressure. On the other hand, for the PS−PLA LBCP, the pancake-like morphology produced at the low pressure transitioned into topologically featureless morphology at the high pressure through the folding of flexible PLA chains. The present study not only complements the well-known models of self-assembly of amphiphilic block copolymers at the air/water interface but also expands the use of the Langmuir−Blodgett technique to hydrophobic block copolymers.

**Acknowledgment.** We gratefully acknowledge the support from the National Science Foundation (NSF CAREER Award, CBET-0844084).

**Supporting Information Available:** Molecular morphologies of PLA and PS arms of BBCP, section analysis of AFM height image of the LB film obtained at $\pi = 5$ mN/m, and AFM height and phase images of Langmuir monolayer at $\pi = 0$ mN/m. This material is available free of charge via the Internet at http://pubs.acs.org.

## References and Notes

(1) Petty, M. C. Cambridge University Press: New York, 1996.
(2) Cheyne, R. B.; Moffitt, M. G. *Langmuir* **2006**, *22*, 8387.
(3) Fasolka, M. J.; Harris, D. J.; Mayes, A. M.; Yoon, M.; Mochrie, S. G. J. *Phys. Rev. Lett.* **1997**, *79*, 3018.
(4) Aksay, I. A.; Trau, M.; Manne, S.; Honma, I.; Yao, N.; Zhou, L.; Fenter, P.; Eisenberger, P. M.; Gruner, S. M. *Science* **1996**, *273*, 892.
(5) Zhu, J.; Eisenberg, A.; Lennox, R. B. *Macromolecules* **1992**, *25*, 6547.
(6) daSilva, A. M. G.; Filipe, E. J. M.; dOliveira, J. M. R.; Martinho, J. M. G. *Langmuir* **1996**, *12*, 6547.
(7) Cheyne, R. B.; Moffitt, M. G. *Langmuir* **2005**, *21*, 5453.
(8) Zhu, J.; Lennox, R. B.; Eisenberg, A. *Langmuir* **1991**, *7*, 1579.
(9) Zhu, J. Y.; Eisenberg, A.; Lennox, R. B. *J. Am. Chem. Soc.* **1991**, *113*, 5583.
(10) Zhu, J.; Hanley, S.; Eisenberg, A.; Lennox, R. B. *Makromol. Chem., Macromol. Symp.* **1992**, *53*, 211.
(11) Cox, J. K.; Yu, K.; Eisenberg, A.; Lennox, R. B. *Phys. Chem. Chem. Phys.* **1999**, *1*, 4417.
(12) Park, J. Y.; Koenen, N.; Forster, M.; Ponnapati, R.; Scherf, U.; Advincula, R. *Macromolecules* **2008**, *41*, 6169.
(13) Francis, R.; Skolnik, A. M.; Carino, S. R.; Logan, J. L.; Underhill, R. S.; Angot, S.; Taton, D.; Gnanou, Y.; Duran, R. S. *Macromolecules* **2002**, *35*, 6483.
(14) Peleshanko, S.; Gunawidjaja, R.; Jeong, J.; Shevehenko, V. V.; Tsukruk, V. V. *Langmuir* **2004**, *20*, 9423.
(15) Peleshanko, S.; Jeong, J.; Gunawidjaja, R.; Tsukruk, V. V. *Macromolecules* **2004**, *37*, 6511.
(16) Genson, K. L.; Hoffman, J.; Teng, J.; Zubarev, E. R.; Vaknin, D.; Tsukruk, V. V. *Langmuir* **2004**, *20*, 904.
(17) Gunawidjaja, R.; Peleshanko, S.; Tsukruk, V. V. *Macromolecules* **2005**, *38*, 8765.
(18) Zhao, L.; Goodman, M. D.; Bowden, N. B.; Lin, Z. Q. *Soft Matter* **2009**, DOI: 10.1039/B912447K.
(19) Peleshanko, S.; Sidorenko, A.; Larson, K.; Villavicencio, O.; Ornatska, M.; McGrath, D. V.; Tsukruk, V. V. *Thin Solid Films* **2002**, *406*, 233.
(20) Njikang, G. N.; Cao, L.; Gauthier, M. *Langmuir* **2008**, *24*, 12919.
(21) Njikang, G. N.; Cao, L.; Gauthier, M. *Macromol. Chem. Phys.* **2008**, *209*, 907.
(22) Seo, Y.; Esker, A. R.; Sohn, D.; Kim, H. J.; Park, S.; Yu, H. *Langmuir* **2003**, *19*, 3313.
(23) Seo, Y.; Im, J. H.; Lee, J. S.; Kim, J. H. *Macromolecules* **2001**, *34*, 4842.
(24) Seo, Y.; Paeng, K.; Park, S. *Macromolecules* **2001**, *34*, 8735.
(25) Lopes, S. I. C.; Goncalves da Silva, A. M. P. S.; Brogueira, P.; Picarra, S.; Martinho, J. M. G. *Langmuir* **2007**, *23*, 9310.
(26) Brinkhuis, R. H. G.; Schouten, A. J. *Macromolecules* **1991**, *24*, 1487.
(27) Tokiwa, Y.; Calabia, B. P. *Appl. Microbiol. Biotechnol.* **2006**, *72*, 244.
(28) Ikada, Y.; Tsuji, H. *Macromol. Rapid Commun.* **2000**, *21*, 117.
(29) Rzayev, J. *Macromolecules* **2009**, *42*, 2135.
(30) Olayo-Valles, R.; Lund, M. S.; Leighton, C.; Hillmyer, M. A. *J. Mater. Chem.* **2004**, *14*, 2729.
(31) Zalusky, A. S.; Olayo-Valles, R.; Wolf, J. H.; Hillmyer, M. A. *J. Am. Chem. Soc.* **2002**, *124*, 12761.
(32) Ho, R. M.; Tseng, W. H.; Fan, H. W.; Chiang, Y. W.; Lin, C. C.; Ko, B. T.; Huang, B. H. *Polymer* **2005**, *46*, 9362.
(33) Nakamura, Y.; Norisuye, T. *Polym. J.* **2001**, *33*, 874.
(34) Wintermantel, M.; Gerle, M.; Fischer, K.; Schmidt, M.; Wataoka, I.; Urakawa, H.; Kajiwara, K.; Tsukahara, Y. *Macromolecules* **1996**, *29*, 978.
(35) Tsukahara, Y.; Namba, S.; Iwasa, J.; Nakano, Y.; Kaeriyama, K.; Takahashi, M. *Macromolecules* **2001**, *34*, 2624.
(36) Rzayev, J.; Hillmyer, M. A. *J. Am. Chem. Soc.* **2005**, *127*, 13373.
(37) Peng, J.; Kim, D. H.; Knoll, W.; Xuan, Y.; Li, B. Y.; Han, Y. C. *J. Chem. Phys.* **2006**, *125*, 064702.
(38) Logan, J. L.; Masse, P.; Dorvel, B.; Skolnik, A. M.; Sheiko, S. S.; Francis, R.; Taton, D.; Gnanou, Y.; Duran, R. S. *Langmuir* **2005**, *21*, 3424.
(39) Kubies, D.; Machova, L.; Brynda, E.; Lukas, J.; Rypacek, F. *J. Mater. Sci.: Mater. Med.* **2003**, *14*, 143.
(40) Fetters, L. J.; Lohse, D. J.; Milner, S. T.; Graessley, W. W. *Macromolecules* **1999**, *32*, 6847.
(41) Dorgan, J. R.; Janzen, J.; Clayton, M. P.; Hait, S. B.; Knauss, D. M. *J. Rheol.* **2005**, *49*, 607.
(42) Numata, K.; Srivastava, R. K.; Finne-Wistrand, A.; Albertsson, A. C.; Doi, Y.; Abe, H. *Biomacromolecules* **2007**, *8*, 3115.
(43) Souheng, W. M. Dekker: New York, 1982.
(44) Devereaux, C. A.; Baker, S. M. *Macromolecules* **2002**, *35*, 1921.